Thermochronologic Data

Table DR1. Summary of new thermochronologic data, along with previously published $^{40}Ar/^{39}Ar$ ages from some of the same samples analyzed in this study.

Table DR2. Summary of thermochronologic data published by other authors and referred to in this study.

GENERAL ASSUMPTION ABOUT THERMOCHRONOLOGIC SYSTEMS

The following assumptions are made for interpreting all applied thermochronologic systems: (1) nominal closure temperatures for the thermochronometers applied; (2) the closure isotherm was horizontal during passage of the sample through its closure temperature; (3) the exhumation path was vertical; and (4) the geothermal gradient stayed constant between the surface and the specific closure temperature. The influence of topography is neglected here, because the large regional extent of the samples analyzed precludes assessment of any local topographic effects on the age distribution.

U-Pb Geochronologic Method for PU1

U-Pb zircon geochronology was conducted at the Arizona LaserChron Center, University of Arizona. Zircons were separated from rock samples using standard crushing and separation techniques, including a water table, magnetic separator and heavy liquids. Individual zircon crystals were then hand-picked under a binocular microscope to select large, inclusion free grains. Approximately 50 grains were then mounted in epoxy and polished to approximately 2/3 of the crystal thickness. The grains were ablated with a New Wave DUV193 Excimer laser, operating at a wavelength of 193 nm and using a spot diameter of 35 microns. The ablated material is then carried in argon gas into the plasma source of a Micromass Isoprobe mmulticollector ICP-MS and ionized. The Micromass Isoprobe is equipped with a flight tube of sufficient width that U, Th, and Pb isotopes are measured simultaneously using nine Faraday collectors, an axial Daly detector, and four ion-counting channels. All measurements were made in static mode, using Faraday detectors for ^{238}U, ^{232}Th, and $^{208-206}Pb$ and an ion-counting channel for ^{204}Pb. ^{235}U is determined from the ^{238}U measurement assuming $^{238}U/^{235}U = 137.88$. Ion yields are ~1 mV per ppm. Each analysis consists of one background run with 20-second integration on peaks and the laser off, 20 1-second integrations with the laser firing, and a 30-second delay to purge for the next analysis. The laser ablates at ~1 micron/second, resulting in an ablation pit ~20 microns in depth. A common lead correction was performed by using the measured ^{204}Pb and assuming an initial Pb composition from Stacey and Kramers (1975) (with uncertainties of 1.0, 0.3, and 2.0 for $^{206}Pb/^{204}Pb$, $^{207}Pb/^{204}Pb$, and $^{208}Pb/^{204}Pb$, respectively). Measurement of ^{204}Pb is unaffected by the presence of ^{204}Hg because backgrounds are measured on peaks (thereby subtracting any background ^{204}Hg and ^{204}Pb) and because very little Hg is present in the argon gas.

The uncertainties in determining $^{206}Pb/^{238}U$ and $^{206}Pb/^{204}Pb$ result in a measurement uncertainty of several percent (at 2-σ level) in the $^{206}Pb^{*}/^{238}U$ age. The low concentrations of ^{207}Pb in younger samples (approximately < 1000 Ma), due to the low concentration of ^{235}U relative to ^{238}U, result in a substantially larger measurement uncertainty for $^{206}Pb/^{207}Pb$. The $^{207}Pb^{*}/^{235}U$ and $^{206}Pb^{*}/^{207}Pb^{*}$ ages for younger grains accordingly have larger uncertainties. Inter-element fractionation of Pb/U is generally <20%, whereas isotopic fractionation of Pb is generally <5%. These fractionations were corrected by analysis of a standard, with a known, concordant ID-TIMS age, between every three unknown analyses. The zircon standards are fragments of a large zircon crystal from a Sri Lankan pegmatite (e.g. Dickinson and Gehrels, 2003) with an age of 564 ± 4 Ma (2σ). The uncertainty resulting from the calibration correction is generally ~3% (2σ) for both $^{207}Pb/^{206}Pb$ and $^{206}Pb/^{238}U$ ages. U and Th concentrations were determined by analyzing a piece of NIST 610 glass with ~500 ppm U and Th and using the resulting measured intensities to calibrate the sample measured U and Th intensities. Additional details about the U-Pb analytical methods are provided in Gehrels et al. (2008).

The crystallization age reported in this paper (69.2 ± 1.4 Ma; Table DR3) is a weighted average of individual, concordant spot analyses using the $^{206}Pb^{*}/^{238}U$ ages, since the $^{207}Pb^{*}/^{235}U$ and $^{207}Pb/^{206}Pb^{*}$ ages are less precise for this young granite. The stated uncertainties (2σ) on the assigned crystallization ages are absolute values and include contributions from all known random and systematic errors. Random errors are included in the data tables. Systematic errors (2σ) are 1.05%. Analyses which have very low $^{206}P/^{204}Pb$ ratios, high ^{204}Pb intensities or very low U concentrations are discarded due to the impractically high uncertainty.

Fig. DR1a is a concordia plot of all the acceptable spot analyses (n = 24); Fig. DR1b shows the weighted mean of the $^{206}Pb^{*}/^{238}U$ ages. All U-Pb plots and weighted average calculations were made using Isoplot 3.00 (Ludwig, 2003).

References

Dickinson, W.R. and Gehrels, G.E., 2003, U-Pb ages of detrital zircons from Permian and Jurassic eolian sandstones of the Colorado Plateau, USA: paleogeographic implications: Sedimentary Geology, v. 163, p. 29-66.

Gehrels, G.E., Valencia, V.A., and Ruiz, J., 2008, Enhanced precision, accuracy, efficiency, and spatial resolution of U-Pb ages by laser ablation-multicollector-inductively coupled plasma-mass spectrometry: Geochemistry, Geophysics, Geosystems, v.9, Q03017, doi:10.1029/2007GC001805.

Ludwig, K.R., 2003, Berkeley Geochronology Center Special Publication No. 4.

Stacey, J.S. and Kramers, J.D., 1975, Approximation of terrestrial lead isotope evolution by a two-stage model: Earth and Planetary Science Letters, v. 26, p. 207-221.

$^{40}Ar/^{39}Ar$ METHODS AND AGE CALCULATIONS

All isotopic data were measured with a MAP-215-50 mass spectrometer equipped with either a Balzers SEV 217 or Johnston electron multiplier. The multipliers are operated at about 1.3 kV or 2.2 kV, respectively and yield a gain above the Faraday collector of about 5000 to 20,000 depending upon source sensitivity. Resolution at 5% peak-height at mass 40 was 450 to 600. Additional information about the New Mexico Geochronology Research Laboratory can be found within New Mexico Bureau of Geology and Mineral Resources open file report OF-AR-1 at:http://geoinfo.nmt.edu/publications/openfile/argon/home.html.

Furnace Step-Heating

The K-feldspar and biotite were step-heated in a double vacuum Mo resistance furnace. Heating times for the K-feldspars were highly variable and are designed to maximize recovery of the diffusion coefficients and to resolve excess argon contamination by performing several isothermal replicate-heating steps (Table DR4). The heating time for biotite was 5 minutes for each step. The samples were gettered during heating using a SAES GP-50 getter operated at ~450°C. Following heating, gas was expanded to a second-stage of the extraction line where it was reacted with 2 GP-50 getters (one at 20°C, one at ~450°C) and a W filament operated at about 2000°C. The K-feldspar gettering time in the second stage was 1-2 minutes, whereas biotite was gettered for 3 minutes. The furnace thermocouple was calibrated by melting copper foil and the recorded temperature underestimated the sample temperature by 15 to 50 °C. For the K-feldspar data, correction of thermocouple temperature to the Cu foil melting point was done and the reported temperature in the data table is calibrated to the foil melting. Estimated accuracy of the heating temperature is ±15 °C for any given step.

Blanks and backgrounds for the K-feldspar were determined during a 15-minute, 800°C blank run. For the long and higher temperature heating steps this method under corrects the true blank and therefore the reported radiogenic yield for these steps contains atmospheric argon that is not solely derived from the samples. However, the blank contribution to the long heating steps is still less than 5% of the total ^{40}Ar signal. Blanks for the biotite were run before, during and after the step heating and typically yielded values of 2×10^{-15}, $4.7\text{x}10^{-18}$, $6\text{x}10^{-18}$, $1.5\text{x}10^{-17}$, and $4.5\text{x}10^{-18}$ moles for masses 40, 39, 38,37 and 36, respectively.

Irradiation, Flux monitoring and Age Calculations

Two irradiations were preformed. Samples from NM-173 were irradiated at the Hamilton, Canada McMaster reactor (position 5C). It was 75 MW hours with samples being irradiated in air while enclosed within an Al vessel. NM-194 samples were irradiated within the central thimble at the USGS Denver Triga reactor for 15 hours. Here, samples were vacuum enclosed within a quartz vessel prior to irradiation.
Fluence gradients were monitored with Fish Canyon (FC-2) sanidine with an assigned age of 28.02 Ma (Renne et al., 1998). Fusing 4-10 individual crystals from each location monitored 4 to 6 locations within individual sample trays. A plane was fit to the weighted mean value of each location and J-factors were determined for the unknowns based on their geometry and the calculated curve. J-factor errors range from 0.1 to 0.17% (1σ). Correction

factors for interfering reactions were measured with K-glass and CaF_2. Typically, 4 to 5 grains of each were fused with the CO_2 laser to obtain a weighted mean value for each correction factor. A plateau age is determined from the inverse variance weighted mean of the chosen steps with the error magnified by the square root of the MSWD for MSWD's greater than 1 (Table DR4). Total gas ages and errors were calculated by quadratically summing isotopic values from each heating step.

K-feldspar Multiple Diffusion Domain (MDD) thermochronology (PU1, JV4)

The determination of a thermal history using the MDD method (Lovera et al., 1989) requires many steps that are outlined below. This is an abbreviated description of the method and more details can be obtained at the New Mexico Bureau of Geology open file report #26 by Sanders and Heizler (2005) or data repository from Sanders et al. (2006). The step-heating schedule is designed to resolve the Arrhenius parameters (e.g. activation energy, diffusion coefficients) of ^{39}Ar transport, a high-resolution age spectrum and to correct of excess argon (Tables DR4). To correct the age spectrum for a characteristic behavior of excess argon release we compare the relationship between apparent age and release of ^{38}Ar derived from chlorine (Harrison et al., 1993; 1994). For sample PU1 K-feldspar there is very minimal excess argon and no correction was required (Figure DR2). For JV4 K-feldspar (Figure DR3) the spectrum has oscillatory age behavior for the first few percent of ^{39}Ar released that was corrected in a fashion outlined by Sanders et al. (2006). A more problematic part of the spectrum is the intermediate age hump (cf. Lovera et al., 2002) between about 10 and 20% of ^{39}Ar released. Here the measured ages are corrected in a somewhat ad hoc fashion prior to MDD modeling by setting the ages to 102 Ma with the large uncertainty shown by the green spectrum in Figure DR3. This is done to prevent the automated modeling process from trying to fit the complex part of the spectrum, but also assumes that the age gradient from about 100 to 110 Ma is accurate.

The diffusion coefficients for ^{39}Ar are calculated for a plane-sheet geometry using the fraction of ^{39}Ar released and time of each heating step. These data are used to construct the Arrhenius and $\log(r/r_o)$ plots (Figures DR2b, DR2c, DR3b, DR3c). The activation energy (E) and initial diffusion coefficient is given by the slope of the low temperature diffusion coefficients on the Arrhenius plot and this Arrhenius law is referred to as r_o. Using these parameters, the entire release of ^{39}Ar for steps at or below 1100 °C are used to determine the diffusion domain distribution. The $\log(r/r_o)$ is simply a different way of viewing the Arrhenius relationship and links the percent of ^{39}Ar to individual diffusion coefficients (Lovera et al., 1991).

Once the domain distribution is determined, the measured age spectrum is forward modeled by inputting thermal histories until a good match is produced between the measured and modeled age spectrum. For this paper we the automated routines (Quidelleur et al., 1997) to deliver a family of thermal histories (Figures DR2d, DR3d).

References

Harrison, T.M., Heizler, M.T., Lovera, O.M., 1993, In vacuo crushing experiments and K-feldspar thermochronometry. Earth. Planet: Science Letters, v. 117, p. 169-180.

Harrison, T.M., Heizler, M.T., Lovera O.M. and Wenji, C., 1994, A chlorine disinfectant for excess argon: Earth Planet. Sci. Lett., v. 123, p. 95-104.

Lovera, O.M., Grove, M., and Harrison, T.M., 2002, Systematic analysis of K-feldspar $^{40}Ar/^{39}Ar$ step-heating results: II. Relevance of laboratory argon diffusion propertiesto nature: Cosmochim. Acta, v. 66, no. 7, p. 1237-1255.
Lovera, O.M., Harrison, T.M., Richter, F.M., 1991, Diffusion domains determined by ^{39}Ar released during step heating: Journal of Geophysical Research, v. 96, p. 2057-2069.
Lovera, O.M., Richter, F.M., Harrison, T.M., 1989, $^{40}Ar/^{39}Ar$ thermochronology for slowly cooled samples having a distribution of domain sizes: Journal of GeophysicalResearch, v. 94, p. 17,917-17,935.
Quidelleur, X., Grove, M., Lovera, O.M., Harrison, T.M., Yin, A., 1997, Thermal evolution and slip history of the Renbu Zedong Thrust, southeastern Tibet: Journal of Geophysical Research, v. 102, n. B2, p. 2659-2679.
Renne, P. R., Swisher, C. C., Deino, A. L., Karner, D. B., Owens, T. L., and DePaolo, D.J., 1998, Intercalibration of standards, absolute ages and uncertainties in $^{40}Ar/^{39}Ar$dating: Chemical Geology, v. 145, no. 1-2, p. 117-152.
Sanders, R.E. and Heizler, M.T., 2005, Extraction of MDD thermal histories from $^{40}Ar/^{39}Ar$ K-feldspar step heating data: NMBGMR Open File Report OF-AR 26.
Sanders, R.E., Heizler, M.T. and Goodwin, L.B., 2006, $^{40}Ar^{39}Ar$ thermochronology constraints on the timing of Proterozoic basement exhumation and fault ancestry,southern Sangre de Cristo Range, New Mexico: Geol. Soc. Am. Bull., v. 118, no.11/12, p. 1489-1506.
Steiger, R. H., and Jäger, E., 1977, Subcommission on geochronology: Convention onthe use of decay constants in geo- and cosmochronology: Earth and Planetary Science Letters, v. 36, p. 359-362.
Taylor, J.R., 1982, An Introduction to Error Analysis: The Study of Uncertainties in Physical Measurements: Univ. Sci. Books, Mill Valley, Calif., 270 p.

APATITE FISSION TRACK THERMOCHRONOLOGY

Apatite Fission Track thermochronology provides information on the timing and rates of cooling occurring at temperature (T) between ca. 60-120 °C, defined as the Partial Annealing Zone (PAZ). The exact T of the upper (hotter) boundary depends on the kinetic characteristics of the apatites and the cooling rate; the former can be quantified by measuring the diameter of track etch pits, known as D_{par} (Donelick et al., 1999; Gallagher et al., 1998; Ketcham et al., 1999). In general, smaller D_{par} are typical of flourine-rich apatites and are characterized by lower temperatures of the upper boundary. Fission track-lengths provide information on the proportion of the cooling history that the sample experienced within the PAZ, and hence how quickly the apatite passed through the PAZ (in the main text we refer to PRZ to include both AFT and AHe annealing zones). Therefore, in order to interpret the AFT data in terms of a T-t path an integrated analysis of fission-track age, track length distribution, and kinetic characteristics of the apatite grains (D_{par}) is necessary. Samples were prepared following standard procedures and analyzed using a drawing tube located above a digitizing tablet and kinetic computer-controlled stage driven by the FTStage program (Dumitru, 1983). Samples were irradiated at Oregon State University. Samples where etched in 5.5 molar nitric acid at 21 °C for 20 seconds. Following irradiation, the mica external detectors were etched with 21 °C in 40% hydrofluoric acid for 45 minutes.

An average of twenty grains for each sample was analyzed for six samples (Figure DR4 and Table DR5). Confined track-lengths, angle between the confined track and the C-crystallographic axis (C-axis projected data), and D_{par} were measured. Use of the angular data mitigates track-measurement bias (Barbarand et al., 2003) and improves annealing model results, as confined tracks anneal anisotropically as a function of orientation (Donelick et al., 1999; Ketcham et al., 1999). All samples pass the χ^2 test (Galbraith and Green, 1990; Green, 1981); therefore, pooled ages, calculated using the Trackkey program (Dunkl, 2002), are reported in Table DR5.

THERMAL MODELING

Thermal modeling was conducted using the HeFTy program (version 1.5.6) (Ketcham, 2005). Five of the six samples analyzed for both AFT and AHe had enough lengths (>50) for modeling and they will be described below. For all samples D_{par} measurements were conducted and used to account for kinetics. More details on modeling parameters are listed in Table DR6. Each model was initiated at a time (t) corresponding to at least double the fission track pooled age of the considered sample so to avoid possible effects of boundary conditions on cooling history. Note that only cooling history between 120 °C and 50 °C are considered significant in the text. A T between 5-20 °C was considered as a representative present-day surface T-window; no extra additional t-T constraints were initially used so to allow the model the highest degree of freedom. (U-Th)/He data were modeled together with AFT data using the Flowers et al. (2009) (to account for alpha damage when possible) and Shuster et al. (2006) methods and the Farley (1996) method for alpha correction. Each model was started by using the youngest He age, and if good or acceptable results were obtained, the second youngest He age was added to the model. Search method: Monte Carlo; 10,000 interactions. For more details on model parameters we refer to Table DR6.

Several tests were run, using different calibrations, for each sample in order to obtain the maximum number of good fits (Fig. DR5). We only report the ones for which we obtained good or acceptable fits. For sample PK3A the only good fit was obtained by modeling FT ages with the youngest He age (47.7 ± 0.9 Ma). For sample PU1 acceptable fits were obtained modeling the two youngest ages (43.8 ± 0.9 and 41.6 ± 0.7 Ma). For sample JV1 good fits were only obtained when using the second youngest He age (45.1 ± 1 Ma), which correlates with the lowest eU (Table DR7). For sample PK1 no fits were obtained when using any He ages for any combination of calibrations/corrections so the modeling results are solely based on AFT data. Sample JV4 does not have enough L for modeling.

References

Barbarand, J., Hurford, A.J., and CArter, A., 2003. Variation in apatite fission-track lenght measurement: implications for thermal history modeelling: Chemical geology, v. 198, p. 77-106.

Donelick, R.A., Ketchman, R.A., and Carlson, W.D., 1999. Varaibility of apatite fission track annealing kinetics: II. Crystallographic orientation effects: American Mineralogist, v. 84, p. 1224-1234.

Dumitru, T.A., 1993. A new computer automated microscope satge system for fission track analysis: Nuclear tracks and radiation measurements, v. 21, p. 575-580.

Dunkl, I., 2002. Trackkey.

Farley, K.A., Wolf, R.A., Silver, L.T., 1996. The effects on long alpha-stopping distances on (U-Th)/He ages: Geochimica et Cosmochimica acta, v. 60, p. 4223-4229

Flowers, R.M., Ketcham, R.A., Shuster, D.L., and Farley, K.A., 2009, Apatite (U–Th)/He thermochronometry using a radiation damage accumulation and annealing model, Geochimica et Cosmochimica Acta, v. 73, p. 2347-2365.

Galbraith, R.F., and Green, P.F., 1990. Estimating the component ages in a finite mixture: Nuclear tracks and radiation measurements, v. 17, p. 197-206.

Gallagher, K., Brown, R., and Johnson, C., 1998. Fission track analysis and its applications to geological problems: Annual Review of Earth and Planetary Sciences, v. 26, p. 519-572.

Green, P.F., 1981. A new look at statistics in fission-track dating: Nuclear tracks and radiation measurements, v. 5, p. 77-86.

Hurford, A.J., and Green, P.F., 1983. The zeta age calibration of fission-track dating: Chemical geology, v. 41, p. 285-317.

Jolivet, M., Brunel, M., Seward, D., Xu, Z., Yang, J., Roger, F., et al., 2001, Mesozoic and Cenozoic tectonics of the northern edge of the Tibetan plateau: fission-track constraints: Tectonophysics, v. 343, p. 111-134, doi: 10.1016/S0040-1951(01)00196-2.

Ketcham, R.A., 2005. Forward and inverse modeling of low-temperature thermochronometry data: Mineral. Soc. Am. Rev. Mineral. Geochem, v. 58, p. 275-314.

Ketcham, R.A., Donelick, R.A., and Carlson, W.D., 1999. Variability of apatite fission-track annealing kinetics: III. Extrapolatio to geological time scales: American Mineralogist, v. 84, p. 1235-1255.

Kirby, E., Reiners, P. W., Krol, M. A., Whipple, K. X., Hodges, K. V., Farley, K. A., et al. 2002, Late Cenozoic evolution of the eastern margin of the Tibetan Plateau: Inferences from 40 Ar/ 39 Ar and (U-Th)/He thermochronology, Tectonics, v. 21, p. 1-19.

Lai, Q., Ding, L., Wang, H., Yue, Y., & Cai, F., 2007, Constraining the stepwise migration of the eastern Tibetan Plateau margin by apatite fission track thermochronology. Science in China Series D: Earth Sciences, v. 50, p. 172-183. doi: 10.1007/s11430-007-2048-7.

Reid, A., Fowler, A., Phillips, D., Wilson, C., 2005, Thermochronology of the Yidun Arc, central eastern Tibetan Plateau: constraints from Ar/Ar K-feldspar and apatite fission track data: Journal of Asian Earth Sciences, v. 25, p. 915-935. doi: 10.1016/j.jseaes.2004.09.002.

Reiners, P.W., Spell, T.L., Nicolescu, S., and Zanetti, K.A., 2004, Zircon (U-Th)/He thermochronometry: He diffusion and comparisons with 40Ar/ 39Ar dating, Geochimica et Cosmochimica Acta, v. 68, p. 1857-1887.

Shuster, D.L., Flowers, R.M., Farley, K.A., 2006. The influence of natural radiation damage on helium diffusion kinetics in apatite: Earth and Planetary science letters, v. 249, p. 148-161

Sobel, E., and Strecker, M.R., 2003. Uplift, exhumation and precipitation: tectonic and climatic control of Late Cenozoic landscape evolution in the northern Sierras Pampeanas, Argentina: Basin Research, v. 15, p. 431-451.

Yuan, W.M., Dong, J.Q., Wang, S.C., Carter, A., 2006, Apatite fissiontrack evidence for Neogene uplift in the eastern Kunlun Mountains, northern Qianghai-Tibet Plateau, China: Journal of Asian Earth Sciences, v. 27, p. 847-856.

(U-Th)/ He METHOD AND CALCULATIONS

Sample Preperation

All sample preparation and analyses were performed at the University of Arizona. Apatite seperates from 17 samples (Table DR7) were extracted by standard separation techniques which include, crushing, sieving, water table, magnetic seperator and the use of heavy liquids (Lithium-Metatungstate and Methylen Iodide). Individual grains were handpicked under a Leica MZ16 stereozoom microscope and checked for inclusion in plane-polarized darkfield. Afterwards inclusion free apatites grains dimensions were measured to apply alpha-ejection corrections. For apatite we assume pinacoidal terminations (Farley et al., 1996; Farley, 2002) at the tips of the crystal. Grains are wrapped in metallic foil for laser heating (House et al., 2002). Apatite is placed in Nb tubing and the ends are pinched closed. We used the approach of single aliquot analysis in our study; usually 2-4 replicates per sample.

He extraction and Measurement

Crystal-bearing foil packets are placed in a Cu or SS planchet, under a KBr coverslip, inside a ~7-cm laser cell pumped to $<10^{-9}$ torr. Aliquots are heated for 3 minutes by a focused beam of a 1-2 W (Nd:YAG) up ~900-1000 °C. If necessary reheating (re-extraction) of single aliquots are preformed to confirm that all ^{4}He has been extracted at least below blank level. Gas released from heated samples is then spiked with 0.1-0.2 pmol ^{3}He, and condensed onto activated charcoal the cold head of a cryogenic trap at 16 K. Helium is then released from the cold head at 37 K into a small volume (~50 cc) with an activated Zr-Ti alloy getter and the source of a Balzers quadrupole mass spectrometer (QMS) with a Channeltron electron multiplier. Peak-centered masses at approximately m/z of 1, 3, 4, and 5.2 are measured. Mass 5.2 establishes background, and mass 1 is used to correct mass 3 for HD and H^{3+}. Corrected ratios of masses 4 to 3 are regressed through ten measurement cycles over 15-60 s to derive an intercept value, which has an uncertainty of 0.05-0.5% over a 4/3 range of $\sim10^{3}$, and compared with the mean corrected ratio to check for significant anomalous changes in the ratio during analysis. Helium contents of unknown samples are calculated by first subtracting the average mass-1-corrected 4/3 measured on multiple procedural blanks analyzed by the same method (a "hotblank"), from the mass-1-corrected 4/3 measured on the unknown. This is then ratioed to the the mass-1-corrected 4/3 measured on a shot of an online reference ^{4}He standard analyzed with the same procedure [minus the mass-1-corrected 4/3 measured on a ^{3}He-only spike shot analyzed using the same procedure as the reference ^{4}He standard (a "lineblank")]. The resulting ratio of measured 4/3's is then multiplied by the moles of ^{4}He delivered in the reference shot. This procedure assumes linearity between measured 4/3 and ^{4}He pressure, which has been confirmed over the the vast majority of the range of ^{4}He contents we analyze by performing multiple replicate analyses of known-age standards with masses and therefore ^{4}He yields ranging over three orders of magnitude. This procedure also relies on the accuracy of the ^{4}He delivery from the reference standard and the precision of its measurement with the ^{3}He spiking procedure. The delivery and its depletion with time are calibrated by multiple capacitance manometry measurements of the volumes of the reference tank and pipette, and the final filling pressure of the tank. Between ~2-5 (depending on the number of unknowns) 4/3 measurements of spiked 4

He reference standards are made each measurement day. Average measured 4/3 of lineblanks (^{3}He spike only) are nearly indistinguishable from that predicted by the purity of the ^{3}He spike (99.75% ^{3}He). Hotblanks, or procedural blanks measured by lasing/heating empty Nb foil packets are typically 0.05-0.1 fmol ^{4}He.

Following degassing apatite grains are dissolved directly in the Nb foil by addition of 20% nitric acid in order to measure the U, Th and Sm of the sample (House et al.,2000). Nb foils with dissolved apatite crystals were then spiked with two different spike solutions, each in 5% HNO_3 solution. The first is 25 or 50 μl of a nominally pure ^{233}U-^{229}Th spike with total U and Th concentrations of 7.55 ± 0.10 ng/ml and 12.3 ± 0.10 ng/ml respectively. The second is 25 or 50 μl of an enriched (97%) ^{147}Sm spike with a total Sm concentration of 10.8 ± 0.10 ng/ml. Following spiking, 200 μl of concentrated SeaStar Baseline HNO_3 is then added to each sample, and the mixture is heated at about 90 °C for two hours. After cooling, the solutions are diluted with 2.5 ml of double-distilled 18 MΩ H_2O, for final spike isotope concentrations of ~0.1-0.2 ppb.

For each sample, including blanks and standards, ^{229}Th, ^{232}Th, ^{233}U, ^{235}U, ^{238}U, ^{147}Sm and ^{152}Sm were measured on a Thermo Finningan Element2. Apatites samples were run with a method using Escan peak jumping with the magnet parked at mass 229.031, sample time 2 ms, 100 samples per peak, mass and averaging windows of 5%, and counting mode, 5 runs and 400 passes for a total of 2000 isotope ratio measurements. Apatite (U-Th)/He ages typically have approximately 1-3% (1σ) error. For more information see also Reiners et al., 2004.

References

Brandon, M.T., Roden-Tice, M.K., and Garver, J.I., 1998. Late Cenozoic exhumation of the Cascadia accretionary wedge in the Olympic Mountains, NW Washington State: Geological Society of America Bulletin, v. 110, no. 8, p. 985-1009

Farley, K.A., 2002. (U-Th)/He Dating: Techniques, Calibrations, and Applications: Reviews in Mineralogy and Geochemistry, v. 47, p. 819-844

Farley, K.A., Wolf, R.A., Silver, L.T., 1996. The effects of long alpha-stopping distances on (U-Th)/He ages: Geochimica et Cosmochimica Acta, v. 60, p. 4223-4229

House, M.A., Kohn, B.P., Farley, K.A., Raza, A., 2002. Evaluating thermal history models for the Otway basin, southeastern Australia, using (U-Th)/He and fission-track data from borehole apatites: Tectonophysics, v.349, p. 277-295

House, M.A., Farley, K.A., Stockli, D., 2000. Helium chronometry of apatite and titanite using Nd-YAG laser heating: Earth and Planetary Science Letters, v. 183, p. 365-368

Reiners, P.W., Spell, T.L., Nicolescu, S., Zanetti, K.A., 2004. Zircon (U-Th)/He thermochronometry: He diffusion and comparision with Ar-40/Ar-39 dating: Geochimica et Cosmochimica Acta, v. 68, p. 1857-1887

Sample #	Long. (E)	Lat. (N)	Elev. (m)	Terrane	Rock type	(U-Pb)-ages (Ma)	40Ar/39Ar-Biotite (Ma)	40Ar/39Ar-Muscovite (Ma)	40Ar/39Ar-MDD K-spar (Ma)	AFT pooled age (Ma)	(U-Th)/He wheighted mean Age (Ma)	AHe-replicates
AR1	33.25	85.19	5506	Qiangtang	Granite	*153 ± 2*[c]					**19.1 ± 0.3**	2
AR2	33.20	86.74	5163	Qiangtang	Granite						**(16.2 ± 4.1)**[a]	1
AR3	33.76	84.56	4923	Qiangtang	Granite						**44.5 ± 2.2**	2
AR4	33.87	84.12	4870	Qiangtang	Granite	*139 ± 9*[d]					**37.0 ± 0.7**	3
AR5	32.78	84.02	4583	Qiangtang	Granite						**48.8 ± 0.7**	2
AR6	32.71	84.24	4609	Qiangtang	Granite						**51.6 ± 2.0**	3
GT1	33.25	85.19	5308	Qiangtang	Granite	**200**					**45.2 ± 1.0**	1
JV1	31.34	89.88	5110	Lhasa	Granite	*125 ± 2*[e]				**61.7 ± 2.9**	**44.8 ± 0.6**	3
JV3	31.50	84.50	4783	Qiangtang	Granite	*79 ± 1*[e]					**44.7 ± 1.1**	2
JV4	31.36	89.89	5230	Lhasa	Granite	*170.7 ± 2.7*[b]	**119.7 ± 0.3**		**96.5**	**53.7 ± 2.6**	**52.0 ± 0.7**	3
PK1A	31.88	91.70	4706	Lhasa	Orthogneiss	*178.8 ± 1.6*[b]	*163.6 ± 0.3*[b]		*119*[b]	**72.9 ± 3.0**	**(121.6 ± 2)**[a]	2
PK1B	31.87	91.70	4706	Lhasa	Orthogneiss					**72.7 ± 4.4**		
PK2	32.03	91.71	4809	Lhasa	Orthogneiss			*166.4 ± 0.4*[b]	*144*[b]	**74.4 ± 3.0**		
PK3	31.41	89.02	4608	Lhasa	Granite	**112 ± 2**					**54.6 ± 1.3**	1
PK3A	32.12	91.71	4762	Lhasa	Orthogneiss	*852 ± 3.5*[b]	*156.5 ± 0.4*[b]		*125*[b]	**71.9 ± 3.1**	**54.4 ± 0.6**	4
PK5	31.50	89.08	4563	Lhasa	Granite	**112 ± 2**					**49.9 ± 0.7**	2
PK6	33.30	85.17	5601	Qiangtang	Granite	*474 ± 4*[c]					**27.6 ± 0.4**	2
PU1	33.25	92.01	5591	Qiangtang	Granitoid	**69.2 ± 1.2**	**68.9 ± 0.1**		**67**	**53.6 ± 2.1**	**43.0 ± 0.5**	3
SH2	30.07	91.14	4533	Lhasa	Granite	*51.9 ± 2.5*[f]					**14.7 ± 0.2**	4

Lat.- Latitude; Long. - Longitude; Elev.- Elevation;

[a] excluded from study due to poor reproducibility

Ages taken from: [b]Gyunn et al, 2006; [c]Pullen et al, in press; [d]Kapp et al., 2003b; [e]Volkmer, unpublished; [f]He et al., 2007

K-feldspar ages correspond to temperatures in the 225-200°C range where the resolved thermal histories are tightly constrained.

Bold letter- new data; italic letter- data from other studies

Sample #	Lat. (E)	Long. (N)	Elev. (m)	Method	Age (Ma)	Err (1s)	Source
93-3	31.111	103.288		(U-Th)/He	4.6	0.4	Kirby et al., 2002
97-2	32.613	103.065		(U-Th)/He	13.4	0.4	Kirby et al., 2002
97-4	32.540	102.900		(U-Th)/He	19.9	0.6	Kirby et al., 2002
97-5	32.550	102.672		(U-Th)/He	20.6	0.6	Kirby et al., 2002
97-6	32.481	102.598		(U-Th)/He	8.2	0.3	Kirby et al., 2002
97-14	32.855	103.925		(U-Th)/He	3.2	0.3	Kirby et al., 2002
98-17	28.199	102.093	1650	(U-Th)/He	17.0	6.7	Clark et al., 2005
98-18	27.712	102.132	1750	(U-Th)/He	19.5	2.1	Clark et al., 2005
98-19	27.706	102.096	2200	(U-Th)/He	18.2	1.5	Clark et al., 2005
98-9	29.172	102.387	1050	(U-Th)/He	5.1	3.2	Clark et al., 2005
98-10	29.147	102.360	1150	(U-Th)/He	17.0	6.5	Clark et al., 2005
98-11	29.128	102.341	1200	(U-Th)/He	18.1	1.8	Clark et al., 2005
98-12	29.089	102.340	1450	(U-Th)/He	21.0	6.0	Clark et al., 2005
01-11	31.198	101.930	2840	(U-Th)/He	8.1	1.2	Clark et al., 2005
01-12	31.195	101.926	2580	(U-Th)/He	6.1	0.5	Clark et al., 2005
01-13	31.194	101.924	2500	(U-Th)/He	5.7	0.1	Clark et al., 2005
01-14	31.204	101.929	3000	(U-Th)/He	9.4	1.7	Clark et al., 2005
01-15	31.173	101.932	2100	(U-Th)/He	5.5	0.3	Clark et al., 2005
01-37	29.645	100.353	3860	(U-Th)/He	50.0	0.6	Clark et al., 2005
01-38	29.635	100.345	3980	(U-Th)/He	60.1	11.1	Clark et al., 2005
01-40	29.574	100.317	4200	(U-Th)/He	112.3	16.4	Clark et al., 2005
01-41	29.532	100.276	4500	(U-Th)/He	111.9	21.2	Clark et al., 2005
01-42	29.516	100.270	4640	(U-Th)/He	92.3	24.1	Clark et al., 2005
01-43	29.461	100.196	4620	(U-Th)/He	91.4	2.2	Clark et al., 2005
01-44	29.358	100.126	4420	(U-Th)/He	101.7	27.2	Clark et al., 2005
01-49	30.124	101.532	4000	(U-Th)/He	57.6	2.7	Clark et al., 2005
01-25	28.543	101.751	1700	(U-Th)/He	4.6	0.8	Clark et al., 2005
01-26	28.534	101.748	1620	(U-Th)/He	10.8	1.6	Clark et al., 2005
01-27	28.552	101.734	1950	(U-Th)/He	5.0	1.2	Clark et al., 2005
01-29	28.835	101.603	2550	(U-Th)/He	8.3	1.4	Clark et al., 2005
01-30	28.874	101.573	2750	(U-Th)/He	10.1	4.5	Clark et al., 2005
01-11	31.198	101.930	2840	AFT	8.4	0.9	Clark et al., 2005
01-12	31.195	101.926	2580	AFT	10.0	0.7	Clark et al., 2005
01-13	31.194	101.924	2500	AFT	10.4	0.7	Clark et al., 2005
01-14	31.204	101.929	3000	AFT	10.5	1.1	Clark et al., 2005
01-15	31.173	101.932	2100	AFT	8.9	0.5	Clark et al., 2005
01-25	28.543	101.751	1700	AFT	5.6	1.0	Clark et al., 2005
01-26	28.534	101.748	1620	AFT	6.4	1.1	Clark et al., 2005
01-27	28.552	101.734	1950	AFT	4.7	1.3	Clark et al., 2005
wbo-04-32C	31.387	101.913	3700	(U-Th)/He	27.7	11.9	Ouimet et al., 2010
wbo-03-20B	31.378	101.921	3200	(U-Th)/He	16.3	3.1	Ouimet et al., 2010
wbo-03-20C	31.374	101.927	3000	(U-Th)/He	8.2	1.5	Ouimet et al., 2010
wbo-03-20D	31.371	101.936	2800	(U-Th)/He	8.4	1.9	Ouimet et al., 2010
wbo-03-20E	31.371	101.942	2600	(U-Th)/He	6.6	0.3	Ouimet et al., 2010
wbo-04-41C	29.460	101.244	4000	(U-Th)/He	5.6	0.8	Ouimet et al., 2010
wbo-04-41A	29.448	101.240	3700	(U-Th)/He	4.7	0.2	Ouimet et al., 2010
wbo-04-16A	29.431	101.235	3100	(U-Th)/He	3.6	0.5	Ouimet et al., 2010
wbo-04-41E	29.420	101.227	2800	(U-Th)/He	1.7	0.5	Ouimet et al., 2010
wbo-04-15	29.484	99.073	3100	(U-Th)/He	9.0	0.7	Ouimet et al., 2010

wbo-04-14	29.482	99.069	2900	(U-Th)/He	8.8	1.5	Ouimet et al., 2010
wbo-04-13	29.480	99.068	2700	(U-Th)/He	7.8	1.8	Ouimet et al., 2010
wbo-04-10	29.414	99.061	2350	(U-Th)/He	7.2	0.1	Ouimet et al., 2010
YA13	28.440	98.940	3320	AFT	42.0	4.0	Reid et al., 2005
YA05	29.460	100.190	4680	AFT	88.7	7.3	Reid et al., 2005
YA04	29.530	100.280	4640	AFT	72.3	7.0	Reid et al., 2005
YA03	29.530	100.280	4490	AFT	85.5	10.9	Reid et al., 2005
YA02	29.600	100.320	4160	AFT	82.3	16.0	Reid et al., 2005
YA32	30.260	99.440	3900	AFT	16.8	1.8	Reid et al., 2005
2003T79	31.177	99.785	4280	AFT	124.3	8.6	Lai et al., 2007
2003T75	31.208	99.758	4402	AFT	151.7	10.4	Lai et al., 2007
2003T76	31.222	99.845	4477	AFT	150.2	10.2	Lai et al., 2007
2003T77	31.264	99.872	4567	AFT	153.7	10.2	Lai et al., 2007
2003T141	29.643	100.352	3845	AFT	81.6	5.8	Lai et al., 2007
2003T142	29.632	100.345	3966	AFT	104.0	7.1	Lai et al., 2007
2003T143	29.616	100.332	4122	AFT	115.0	7.6	Lai et al., 2007
2003T144	29.543	100.283	4477	AFT	115.0	4.0	Lai et al., 2007
2003T145	29.532	100.283	4488	AFT	114.0	7.5	Lai et al., 2007
2003T150	29.255	100.086	4272	AFT	154.9	10.6	Lai et al., 2007
FT93-139			600	AFT	162.0	23.0	Arne et al., 1997
FT93-140			600	AFT	189.0	20.0	Arne et al., 1997
FT93-143			750	AFT	33.0	8.0	Arne et al., 1997
FT93-144			1450	AFT	72.0	7.0	Arne et al., 1997
FT93-145			1200	AFT	73.0	14.0	Arne et al., 1997
FT93-149			3150	AFT	57.0	12.0	Arne et al., 1997
FT93-150			3050	AFT	38.0	11.0	Arne et al., 1997
FT93-151			4050	AFT	122.0	122.0	Arne et al., 1997
FT-1			3950	AFT	6.6	2.0	Arne et al., 1997
FT-2			3500	AFT	7.3	2.8	Arne et al., 1997
FT-4			2750	AFT	3.9	1.2	Arne et al., 1997
FT-5			2400	AFT	3.8	2.6	Arne et al., 1997
FT-7			950	AFT	6.5	2.4	Arne et al., 1997
CW-6a			1150	AFT	4.8	3.0	Arne et al., 1997
CW-3			800	AFT	173.0	17.0	Arne et al., 1997
CW-14			800	AFT	140.0	24.0	Arne et al., 1997
FT93-152			800	AFT	39.0	10.0	Arne et al., 1997
FT93-154			900	AFT	168.0	20.0	Arne et al., 1997
CW-31			1200	AFT	108.0	23.0	Arne et al., 1997
CW-33			800	AFT	93.0	28.0	Arne et al., 1997
CW-51				AFT	105.0	17.0	Arne et al., 1997
CW-52			1100	AFT	14.0	3.0	Arne et al., 1997
CW-39b				AFT	4.3	1.4	Arne et al., 1997
CW-36			1250	AFT	8.9	8.0	Arne et al., 1997
CW-40				AFT	11.0	7.0	Arne et al., 1997
WQ122	38.450	94.775	4000	AFT	20.7	2.3	Jolivet et al., 2001
AT131	37.630	91.363	3400	AFT	17.6	1.5	Jolivet et al., 2001
AT118	36.060	90.225	5500	AFT	17.3	1.8	Jolivet et al., 2001
AT113	36.700	89.263	5000	AFT	19.3	1.8	Jolivet et al., 2001
AT103	36.990	88.813	4377	AFT	52.8	7.2	Jolivet et al., 2001
TGL-Ft-1	33.009	91.973	5040	AFT	47.3	4.0	Wang et al., 2008

YSP-Ft-1	33.603	92.078	4660	AFT	37.7	3.0	Wang et al., 2008
TFt-1	34.372	92.508	4729	AFT	48.9	5.3	Wang et al., 2008
FFt-1	34.693	92.907	4900	AFT	51.2	12.8	Wang et al., 2008
FFt-2	34.675	92.920	4930	AFT	115.0	12.2	Wang et al., 2008
EFt-1	34.613	92.759	4760	AFT	32.9	4.8	Wang et al., 2008
WLFt-y3	34.597	90.174	5100	AFT	52.6	4.5	Wang et al., 2008
WLFt-y2	34.598	90.175	5080	AFT	56.5	11.3	Wang et al., 2008
WLFt-y0	34.600	90.173	5050	AFT	44.2	4.7	Wang et al., 2008
FP04-9-Ft	34.525	92.726	4590	AFT	43.6	4.3	Wang et al., 2008
KL-2	35.550	93.970	4694	AFT	72.7	9.8	Wang et al., 2008
KL-4	35.550	93.970	4711	AFT	70.3	7.3	Wang et al., 2008
KL-1	35.550	93.970	4690	AFT	61.5	12.4	Wang et al., 2008
P0126HX	33.607	92.067	4690	AFT	38.2	4.0	Wang et al., 2008
P0158HX	33.600	92.067	4700	AFT	47.3	4.3	Wang et al., 2008
P0171HX	33.580	92.067	4720	AFT	39.4	5.5	Wang et al., 2008
P01(96)B1	33.600	92.067	4722	AFT	82.0	18.7	Wang et al., 2008
P172FT5	33.450	92.350	5350	AFT	65.2	9.9	Wang et al., 2008
P172FT2	33.450	92.350	5550	AFT	55.8	5.4	Wang et al., 2008
P171FT1	33.450	92.350	5640	AFT	55.5	7.5	Wang et al., 2008
P1407B1	34.978	90.022	4930	AFT	93.1	25.5	Wang et al., 2008
SP17-(01)B1	34.520	92.900	5050	AFT	47.2	5.9	Wang et al., 2008
P03-11B2	34.630	91.120	5080	AFT	46.7	2.7	Wang et al., 2008
P14-51	34.978	90.022	4930	AFT	40.0	5.5	Wang et al., 2008
SQ16	34.574	92.912	5350	AFT	39.4	4.2	Wang et al., 2008
P14-52	34.978	90.022	4930	AFT	39.1	4.6	Wang et al., 2008
SP19-1	34.560	92.905	5100	AFT	37.4	4.5	Wang et al., 2008
SQ22	34.574	92.912	5350	AFT	36.2	4.3	Wang et al., 2008
KP01-(21)C2	35.429	90.785	5200	AFT	28.6	2.8	Wang et al., 2008
P03-15B	34.630	91.120	5080	AFT	22.9	3.4	Wang et al., 2008
PC59	29.270	91.120	3700	AFT	6.9	0.9	Copeland et al., 1995
K-88-73	29.300	90.740	3440	AFT	20.0	1.6	Copeland et al., 1995
PC-88-65	29.310	91.470	3750	AFT	24.9	2.3	Copeland et al., 1995
H-88-1	29.350	90.740	3800	AFT	18.6	1.5	Copeland et al., 1995
PC-88-32	29.420	90.910	4560	AFT	18.1	1.7	Copeland et al., 1995
M370	29.490	90.950	4350	AFT	16.2	1.2	Copeland et al., 1995
K-88-66	29.560	91.300	5050	AFT	33.3	5.2	Copeland et al., 1995
PC-88-39	29.690	90.930	3750	AFT	19.9	1.8	Copeland et al., 1995
K-88-33	29.880	90.730	3870	AFT	45.2	5.9	Copeland et al., 1995
PC-88-29	30.090	90.570	4300	AFT	9.5	0.9	Copeland et al., 1995
PK05-16	35.083	75.078	3432	AFT	14.6	1.1	van der Beek et al., 2009
PK05-16	35.083	75.078	3432	(U-Th)/He	8.5	0.9	van der Beek et al., 2009
PK05-17	35.024	75.155	3689	AFT	21.6	1.6	van der Beek et al., 2009
PK05-20	35.016	75.431	3961	AFT	20.7	1.2	van der Beek et al., 2009
PK05-28	35.120	75.591	3501	AFT	27.0	3.5	van der Beek et al., 2009
PK05-29	35.141	75.605	3291	AFT	23.6	2.4	van der Beek et al., 2009
PK05-30	35.153	75.611	3128	AFT	21.2	2.4	van der Beek et al., 2009
PK05-31	35.252	75.641	2594	AFT	22.6	2.8	van der Beek et al., 2009
PK05-36	35.174	75.619	2960	(U-Th)/He	10.6	2.4	van der Beek et al., 2009
PK05-50	35.091	75.753	3991	AFT	23.1	1.9	van der Beek et al., 2009
PK05-50	35.091	75.753	3991	(U-Th)/He	9.7	0.6	van der Beek et al., 2009

PK05-51	35.118	75.793	3481	AFT	19.0	2.3	van der Beek et al., 2009
PK05-54	35.129	75.940	2534	AFT	15.4	1.5	van der Beek et al., 2009
XT41			4292	AFT	48.0	3.0	Yuang et al., 2006
XT35			3806	AFT	45.0	2.0	Yuang et al., 2006
XT34			3804	AFT	39.0	2.0	Yuang et al., 2006
XT33			3806	AFT	45.0	2.0	Yuang et al., 2006
XT31			3768	AFT	44.0	2.0	Yuang et al., 2006
XT28			3707	AFT	38.0	2.0	Yuang et al., 2006
XT51			3614	AFT	25.0	2.0	Yuang et al., 2006
XT17-1			3513	AFT	27.0	6.0	Yuang et al., 2006
XT19			3490	AFT	27.0	2.0	Yuang et al., 2006
XT20			3450	AFT	30.0	2.0	Yuang et al., 2006
XT15			3467	AFT	28.0	3.0	Yuang et al., 2006
H-23	31.423	89.805		AFT	59.4	2.3	Hetzel et al., 2011
H-24	31.443	89.805		AFT	58.5	3.3	Hetzel et al., 2011
H-29	31.443	89.898		AFT	56.8	2.8	Hetzel et al., 2011
H-30	31.468	89.896		AFT	58.2	3.0	Hetzel et al., 2011
H-31	31.479	89.919		AFT	68.4	3.9	Hetzel et al., 2011
DC-31	31.467	89.921		AFT	58.8	3.0	Hetzel et al., 2011
DC-33	31.373	90.014		AFT	59.6	2.4	Hetzel et al., 2011
H-23	31.423	89.805		(U-Th)/He	56.2	0.9	Hetzel et al., 2011
H-24	31.443	89.805		(U-Th)/He	56.3	0.7	Hetzel et al., 2011
H-29	31.443	89.898		(U-Th)/He	53.6	1.2	Hetzel et al., 2011
H-30	31.468	89.896		(U-Th)/He	59.0	3.6	Hetzel et al., 2011
H-31	31.479	89.919		(U-Th)/He	55.4	5.7	Hetzel et al., 2011
DC-31	31.467	89.921		(U-Th)/He	55.1	3.3	Hetzel et al., 2011
DC-33	31.373	90.014		(U-Th)/He	52.0	0.2	Hetzel et al., 2011

Lat- Latitude; Long. - Longitude; Elev. -Elevation;
AFT- Apatite Fissiontrack; (U-Th)/He- Apatite Helium-dating

U-Pb References

Dickinson, W.R. and Gehrels, G.E., 2003. U-Pb ages of detrital zircons from Permian and Jurassic eolian sandstones of the Colorado Plateau, USA: paleogeographic implications. Sedimentary Geology, 163(1-2): 29-66.

Ludwig, K.R., 2003. Berkeley Geochronology Center Special Publication No. 4.

Stacey, J.S. and Kramers, J.D., 1975. Approximation of terrestrial lead isotope evolution by a two-stage model. Earth and Planetary Science Letters, 26(2): 207-221.

Table DR3 – U-Pb data for PU1

				Isotopic ratios					Apparent ages (Ma)					
Sample spot	U (ppm)	$^{206}Pb/^{204}Pb$	U/Th	$^{207}Pb^*/^{235}U$	± (%)	$^{206}Pb^*/^{238}U$	± (%)	error corr	$^{206}Pb^*/^{238}U$	± (Ma)	$^{207}Pb^*/^{235}U$	± (Ma)	$^{206}Pb^*/^{207}Pb^*$	± (Ma)
1C	809	2839	0.8	0.07890	16.11	0.01077	2.22	0.138	69	1.5	77	12.0	334	364
2C	270	912	1.2	0.05700	55.63	0.01209	4.80	0.086	77	3.7	56	30.5	-773	1675
5C	445	914	0.7	0.10230	23.91	0.01227	2.56	0.107	79	2.0	99	22.5	621	520
7C	2591	3901	1.8	0.07470	6.04	0.01091	1.32	0.219	70	0.9	73	4.3	179	138
8C	2107	5641	0.9	0.06650	7.20	0.01033	1.72	0.239	66	1.1	65	4.6	34	168
11C	259	128	2.5	0.11662	38.49	0.01170	7.55	0.196	75	5.6	112	40.8	994	795
13C	1049	1827	3.4	0.11449	47.74	0.01085	1.13	0.024	70	0.8	110	49.8	1110	1014
14C	399	870	0.9	0.07962	24.63	0.01021	4.53	0.184	65	3.0	78	18.4	475	543
15C	583	991	1.0	0.07610	27.48	0.01097	2.83	0.103	70	2.0	74	19.7	210	644
16T	352	946	1.6	0.09090	32.96	0.01074	4.67	0.142	69	3.2	88	27.9	653	718
17T	546	666	1.0	0.10227	50.75	0.01216	7.99	0.157	78	6.2	99	47.8	639	1150
18T	407	2506	1.5	0.11120	22.94	0.01169	3.72	0.162	75	2.8	107	23.3	899	473
19T	506	2224	1.7	0.07856	26.30	0.01092	3.78	0.144	70	2.6	77	19.5	293	603
20T	546	535	1.3	0.07819	12.70	0.01017	1.46	0.115	65	0.9	76	9.3	444	281
21T	412	1822	1.5	0.09208	17.61	0.01110	1.96	0.111	71	1.4	89	15.1	608	381
22T	493	2172	1.9	0.09422	21.04	0.01127	2.23	0.106	72	1.6	91	18.4	626	456
23T	550	2224	2.2	0.07497	27.00	0.01188	3.42	0.127	76	2.6	73	19.1	-15	658
24T	1092	5173	1.6	0.07843	11.34	0.01071	1.46	0.128	69	1.0	77	8.4	333	256
25T	601	2990	1.4	0.08500	18.98	0.01037	2.02	0.106	66	1.3	83	15.1	584	413
26T	438	756	1.7	0.07692	32.45	0.01119	4.25	0.131	72	3.0	75	23.5	188	766
27T	604	3555	1.5	0.08199	18.52	0.01061	2.80	0.151	68	1.9	80	14.2	454	409
28T	360	783	1.5	0.08921	49.20	0.01124	3.88	0.079	72	2.8	87	40.9	513	1145
29T	384	1766	1.7	0.09893	25.90	0.01128	4.68	0.181	72	3.4	96	23.7	728	548
30T	756	1510	1.7	0.11421	16.06	0.01058	2.22	0.138	68	1.5	110	16.7	1154	318

Table DR4. Argon isotopic data and age assignments.

	ID	Temp (°C)	$^{40}Ar/^{39}Ar$	$^{37}Ar/^{39}Ar$	$^{36}Ar/^{39}Ar$ (x 10^{-3})	$^{39}Ar_K$ (x 10^{-15} mol)	K/Ca	$^{40}Ar^*$ (%)	^{39}Ar (%)	Age (Ma)	±1σ (Ma)	Time (min)
	PU1, Biotite, 5.21 mg, J=0.0036038±0.13%, D=1.003±0.001, NM-194B, Lab#=56112-01											
x	A	640	39.52	0.1349	105.8	2.76	3.8	20.9	0.6	52.9	2.3	
	B	740	17.25	0.0172	22.09	17.9	29.7	62.2	4.5	68.36	0.61	
	C	840	12.07	0.0053	4.132	86.5	96.7	89.9	23.1	69.15	0.14	
	D	910	11.11	0.0032	1.212	91.2	158.5	96.8	42.7	68.53	0.14	
	E	990	11.13	0.0095	1.360	31.2	53.7	96.4	49.5	68.38	0.28	
	F	1065	11.27	0.0262	1.566	44.9	19.5	95.9	59.1	68.91	0.13	
	G	1100	11.50	0.0300	2.282	49.8	17.0	94.2	69.9	69.00	0.12	
	H	1170	11.66	0.0666	2.771	88.5	7.7	93.0	88.9	69.10	0.13	
	I	1200	11.47	0.0470	2.370	46.6	10.9	93.9	99.0	68.67	0.14	
	J	1240	11.56	0.0256	3.129	4.83	19.9	92.0	100.0	67.80	0.69	
	Integrated age ± 1σ		n=10			464.1	18.8	K2O=9.50%		68.74	0.14	
	Plateau ± 1σ	steps B-J	n=9	MSWD=2.80		461.4			99.4	68.87	0.13	
	JV4, Biotite, 4.96 mg, J=0.003657±0.17%, D=1.002±0.001, NM-194E, Lab#=56146-01											
x	A	640	14.54	0.0641	26.62	6.19	8.0	45.9	1.4	43.49	0.90	
x	B	740	19.17	-0.0003	1.887	48.2	-	97.1	12.0	118.72	0.29	
x	C	840	19.02	0.0014	0.7691	120.6	362.3	98.8	38.5	119.85	0.23	
x	D	910	19.45	0.0090	0.8261	46.6	56.5	98.8	48.7	122.42	0.31	
x	E	990	19.82	0.0171	0.8646	57.4	29.8	98.7	61.4	124.65	0.23	
x	F	1065	18.98	0.0134	0.2577	112.9	38.0	99.6	86.2	120.56	0.19	
x	G	1100	18.93	0.0239	0.3831	28.46	21.4	99.4	92.4	120.02	0.24	
x	H	1170	18.89	0.1218	0.0037	24.27	4.2	100.1	97.8	120.53	0.25	
x	I	1200	18.87	0.1466	1.399	6.68	3.5	97.9	99.3	117.88	0.69	
x	J	1240	20.07	0.0777	7.934	3.38	6.6	88.3	100.0	113.3	1.1	
	Integrated age ± 1σ		n=10			454.8	27.8	K2O=9.63%		119.73	0.25	
	Plateau ± 1σ	no plateau										

Table DR4. Argon isotopic data and age assignments.

ID	Temp (°C)	$^{40}Ar/^{39}Ar$	$^{37}Ar/^{39}Ar$	$^{36}Ar/^{39}Ar$ (x 10^{-3})	$^{39}Ar_K$ (x 10^{-15} mol)	K/Ca	$^{40}Ar^*$ (%)	^{39}Ar (%)	Age (Ma)	±1σ (Ma)	Time (min)
PU1, K-Feldspar, 15.72 mg, J=0.0036097±0.14%, D=1.002±0.001, NM-194B, Lab#=56111-01											
B	450	557.2	0.1496	1834.4	1.39	3.4	2.7	0.1	96.0	15.5	10.7
C	450	162.5	0.1835	505.1	0.532	2.8	8.2	0.1	84.5	7.9	20.9
D	500	61.75	0.0929	173.6	1.02	5.5	16.9	0.2	66.8	3.4	9.9
E	500	30.88	0.0758	71.35	1.47	6.7	31.7	0.3	62.7	2.1	20.4
F	550	26.39	0.0556	55.25	2.92	9.2	38.1	0.6	64.3	1.2	9.1
G	550	15.03	0.0515	16.47	3.97	9.9	67.6	0.9	64.99	0.69	20.0
H	600	22.58	0.0657	41.01	9.39	7.8	46.3	1.6	66.86	0.59	12.1
I	600	12.14	0.0591	5.951	8.44	8.6	85.5	2.3	66.34	0.32	22.1
J	650	15.12	0.0500	15.56	13.7	10.2	69.6	3.3	67.21	0.35	12.0
K	650	11.53	0.0408	3.615	13.6	12.5	90.8	4.4	66.85	0.22	22.1
L	700	12.52	0.0373	6.323	14.4	13.7	85.1	5.5	68.01	0.23	12.0
M	700	11.00	0.0308	1.571	19.8	16.6	95.8	7.0	67.28	0.17	22.2
N	750	12.21	0.0302	5.611	26.0	16.9	86.4	9.0	67.43	0.18	11.8
O	750	11.09	0.0230	1.765	26.5	22.2	95.3	11.1	67.52	0.15	22.0
P	800	11.88	0.0198	4.500	32.4	25.8	88.8	13.6	67.40	0.16	12.5
Q	800	11.22	0.0172	1.964	23.9	29.7	94.8	15.4	67.95	0.16	22.6
R	850	12.18	0.0161	5.090	24.6	31.8	87.6	17.3	68.16	0.19	12.4
S	850	11.19	0.0130	2.095	27.2	39.2	94.5	19.4	67.49	0.15	22.5
T	900	13.12	0.0124	8.289	30.6	41.0	81.3	21.8	68.13	0.19	12.8
U	900	12.06	0.0120	4.989	27.0	42.5	87.8	23.9	67.62	0.17	22.9
V	950	15.20	0.0116	15.26	37.9	44.1	70.3	26.8	68.24	0.24	12.7
W	950	13.77	0.0086	10.22	30.6	59.2	78.0	29.2	68.60	0.21	22.8
X	1000	15.99	0.0105	17.62	58.7	48.7	67.4	33.7	68.85	0.23	12.8
Y	1000	14.38	0.0086	12.28	61.9	59.3	74.8	38.5	68.61	0.19	22.8
Z	1050	14.96	0.0085	14.08	110.6	60.4	72.2	47.0	68.91	0.19	12.8
AA	1050	13.28	0.0094	8.637	66.2	54.0	80.8	52.1	68.49	0.16	22.8
AB	1100	13.60	0.0119	9.580	101.9	43.0	79.2	60.0	68.72	0.16	12.8
AC	1100	13.03	0.0119	7.631	85.1	43.0	82.7	66.6	68.79	0.15	22.8
AD	1100	12.77	0.0089	6.813	100.4	57.3	84.2	74.4	68.67	0.14	56.8
AE	1100	12.73	0.0071	6.655	99.1	71.5	84.5	82.0	68.69	0.14	116.8
AF	1200	12.78	0.0056	6.479	71.1	91.2	85.0	87.5	69.34	0.15	6.7
AG	1250	13.54	0.0067	9.249	62.9	75.7	79.8	92.4	68.98	0.17	6.6
AH	1350	13.52	0.0107	8.730	38.2	47.5	80.9	95.3	69.83	0.18	7.0
AI	1690	13.28	0.0143	8.012	60.3	35.7	82.2	100.0	69.64	0.16	3.0
Integrated age ± 1σ			n=34		1293.7	37.5	K2O=8.76%		68.57	0.18	

Table DR4. Argon isotopic data and age assignments.

ID	Temp (°C)	$^{40}Ar/^{39}Ar$	$^{37}Ar/^{39}Ar$	$^{36}Ar/^{39}Ar$ (x 10^{-3})	$^{39}Ar_K$ (x 10^{-15} mol)	K/Ca	$^{40}Ar*$ (%)	^{39}Ar (%)	Age (Ma)	±1σ (Ma)	Time (min)
JV4, K-Feldspar, 15.56 mg, J=0.0036288±0.12%, D=1.002±0.001, NM-194B, Lab#=56119-01											
B	450	254.4	0.0264	431.8	2.37	19.3	49.8	0.2	682.8	3.8	10.9
C	450	68.88	0.0860	164.0	0.729	5.9	29.7	0.2	129.0	4.1	20.9
D	500	74.81	0.0420	44.02	2.44	12.2	82.6	0.4	365.0	1.5	9.8
E	500	19.65	0.0511	15.80	2.34	10.0	76.3	0.5	95.5	1.1	20.5
F	550	37.91	0.0233	18.71	6.51	21.9	85.4	0.9	200.36	0.61	9.1
G	550	14.73	0.0186	3.149	4.92	27.4	93.7	1.2	88.09	0.52	19.9
H	600	21.07	0.0131	6.195	15.7	38.9	91.3	2.2	121.72	0.28	12.0
I	600	14.68	0.0156	1.299	11.8	32.6	97.4	3.0	91.18	0.26	22.3
J	650	16.82	0.0130	3.149	18.5	39.3	94.5	4.1	101.09	0.23	12.0
K	650	15.43	0.0105	0.6780	15.9	48.4	98.7	5.1	97.00	0.21	22.1
L	700	16.43	0.0097	1.751	20.7	52.3	96.9	6.4	101.22	0.20	12.1
M	700	16.22	0.0093	0.4825	18.5	54.6	99.1	7.6	102.26	0.24	22.3
N	750	16.97	0.0093	1.424	22.4	54.8	97.5	9.0	105.16	0.20	11.8
O	750	16.80	0.0110	0.4621	15.3	46.2	99.2	10.0	105.89	0.21	22.1
P	800	17.10	0.0116	1.093	21.7	43.8	98.1	11.4	106.59	0.22	12.4
Q	800	16.97	0.0121	0.4764	17.7	42.3	99.2	12.5	106.86	0.23	22.6
R	850	17.19	0.0136	1.447	17.5	37.5	97.5	13.6	106.50	0.23	12.4
S	850	16.99	0.0092	0.7238	15.7	55.7	98.7	14.6	106.54	0.22	22.5
T	900	17.30	0.0150	2.355	14.2	34.1	96.0	15.5	105.48	0.24	12.8
U	900	16.72	0.0110	1.266	17.6	46.3	97.8	16.6	103.90	0.21	22.9
V	950	17.09	0.0110	3.021	20.8	46.2	94.8	17.9	103.01	0.23	12.7
W	950	16.92	0.0089	2.515	21.7	57.2	95.6	19.3	102.87	0.21	22.8
X	1000	17.51	0.0086	4.799	27.6	59.6	91.9	21.0	102.31	0.20	12.8
Y	1000	17.43	0.0086	4.328	35.9	59.6	92.7	23.3	102.71	0.19	22.9
Z	1050	17.91	0.0132	5.620	51.3	38.5	90.7	26.5	103.28	0.19	12.8
AA	1050	17.74	0.0121	4.756	56.5	42.1	92.1	30.1	103.82	0.17	22.8
AB	1100	17.94	0.0153	4.502	76.3	33.3	92.6	34.9	105.51	0.17	12.8
AC	1100	17.92	0.0132	3.717	69.9	38.7	93.9	39.4	106.85	0.17	22.8
AD	1100	17.83	0.0083	2.767	97.6	61.3	95.4	45.5	107.99	0.15	56.9
AE	1100	17.84	0.0048	2.357	119.1	105.2	96.1	53.1	108.81	0.14	116.8
AF	1200	17.95	0.0025	2.202	153.3	204.4	96.4	62.8	109.78	0.14	6.6
AG	1250	18.13	0.0012	1.807	338.8	442.5	97.1	84.2	111.60	0.15	6.6
AH	1350	18.16	0.0023	1.795	152.5	224.9	97.1	93.9	111.82	0.15	6.9
AI	1690	18.40	0.0052	1.738	96.9	97.3	97.2	100.0	113.40	0.15	3.0
Integrated age ± 1σ			n=34		1580.3	74.5	K2O=10.75%		110.11	0.18	

Table DR4. Argon isotopic data and age assignments.

ID	Temp (°C)	$^{40}Ar/^{39}Ar$	$^{37}Ar/^{39}Ar$	$^{36}Ar/^{39}Ar$ (x 10^{-3})	$^{39}Ar_K$ (x 10^{-15} mol)	K/Ca	$^{40}Ar^*$ (%)	^{39}Ar (%)	Age (Ma)	±1σ (Ma)	Time (min)

Notes:

Isotopic ratios corrected for blank, radioactive decay, and mass discrimination, not corrected for interfering reactions.

Errors quoted for individual analyses include analytical error only, without interfering reaction or J uncertainties.

Integrated age calculated by summing isotopic measurements of all steps.

Integrated age error calculated by quadratically combining errors of isotopic measurements of all steps.

Plateau age is inverse-variance-weighted mean of selected steps.

Plateau age error is inverse-variance-weighted mean error (Taylor, 1982) times root MSWD where MSWD>1.

Plateau error is weighted error of Taylor (1982).

Decay constants and isotopic abundances after Steiger and Jäger (1977).

x symbol preceding sample ID denotes analyses excluded from plateau age calculations.

Weight percent K_2O calculated from ^{39}Ar signal, sample weight, and instrument sensitivity.

Ages calculated relative to FC-2 Fish Canyon Tuff sanidine interlaboratory standard at 28.02 Ma

Decay Constant (LambdaK (total)) = 5.543e-10/a

D = Mass discrimination. 1 AMU in favor of light isotopes.

Correction factors: NM-194	NM-173
$(^{39}Ar/^{37}Ar)_{Ca}$ = 0.000676 ± 5e-06	$(^{39}Ar/^{37}Ar)_{Ca}$ = 0.00079 ± 2e-05
$(^{36}Ar/^{37}Ar)_{Ca}$ = 0.000276 ± 2e-06	$(^{36}Ar/^{37}Ar)_{Ca}$ = 0.000283 ± 5e-06
$(^{38}Ar/^{39}Ar)_{K}$ = 0.0132	$(^{38}Ar/^{39}Ar)_{K}$ = 0.0124
$(^{40}Ar/^{39}Ar)_{K}$ = 0.01 ± 0.002	$(^{40}Ar/^{39}Ar)_{K}$ = 0.02895 ± 0.00059

Sample code	location	No Xls[a]	Rho-S (e5)[b]	NS[c]	Rho-I	NI[c]	P(χ)[2]	Rho-D (e5)[e]	ND[f]	Age (Ma)	error ± 1σ	U (ppm)	ML (µm) (N)	Error (µm)	SD	D_{par} (µm)	SD
PK1A (PK-97-6-4-1A)	Amdo	20	13.535	1086	34.211	2745	36.18	1.0321	4009	72.9	3.0	42.86	/		/	2.5	0.4
*PK1B (PK-97-6-4-1B)	Amdo	20	20.83	1320	52.422	3322	44.08	1.0245	4009	72.7	4.4	64.1	12.7 N(119)	0.88	1.3	2.0	0.3
*PK2 PK-97-6-4-2)	Amdo	20	11.757	1176	28.692	2870	51.13	1.0169	4009	74.4	3.0	34.75	12.9 N(69)	1.05	1.5	2.0	0.2
*PK3A (PK-97-6-4-3A)	Amdo	20	8.969	982	21.501	2354	54.53	1.0018	4009	71.9	3.1	27.47	13.1 N(70)	1.04	1.4	1.9	0.1
*JV1 (JV61504-1)	Bangge	20	12.876	703	43.446	2372	60.49	1.1488	4773	61.7	2.9	53.81	12.2 N(77)	1.01	1.7	2.2	0.1
JV4 (JV61504-4)	Bangge	20	4.496	682	17.91	2717	66.93	1.152	4773	53.7	2.6	19.83	13.1 N(35)		1.5	2.0	0.1
*PU1	Tangulla	20	9.681	1227	31.837	4035	88.51	0.9715	4009	53.6	2.1	41.34	12.6 N(106)	1.08	0.1	1.7	0.1

Table DR5. AFT analytical data. Samples analyzed with a Leica DMRM microscope with drawing tube located above a digitizing tablet and a Kinetek computer-controlled stage driven by the FTStage program (Dumitru, 1993).

Analysis performed with reflected and transmitted light at 1250x magnification. Samples were irradiated at Oregon State University. Samples where etched in 5.5 molar nitric acid at 21°C for 20 seconds. Following irradiation, the mica external detectors were etched with 21°C in 40% hydrofluoric acid for 45 minutes. The pooled age is reported for all samples as they pass the χ^2 test, suggesting that they represent a single population. Error is one σ, calculated using the zeta calibration method (Hurford and Green, 1983) with zeta of 358.97 ± 4.42 for apatite [unpublished data, 2006, *B. Carrapa*]. *Modeled samples.

[a]No Xls is the number of individual crystals dated.
[b]Rho-S and Rho-I are the spontaneous and induced track density measured, respectively (tracks/cm^2).
[c]NS and NI are the number of spontaneous and induced tracks counted, respectively.
$(\chi)^2$ (%) is the chi-square probability (Galbraith and Green, 1990; Green, 1981). Values greater than 5% are considered to pass this test and represent a single population of ages.
[e]Rho-D is the induced track density in external detector adjacent to CN5 dosimetry glass (tracks/cm^2).
[f]ND is the number of tracks counted in determining Rho-D.

D_{par}: fission track etch pit measurements; SD is the related standard deviation. ML: mean track length; SD: standard deviation. N(x): number of length measurements. *are the modeled samples.

/: no data.

	AFT* model parameter	AHe model parameter	T-t constraints	Number of fits	AHe age	error	Info
PK3	Annealing model: Kectahm et al. (2007)	AHe calibration: Flowers et al. (in press)	maximum T: 120^{o}C	Acceptable: 41	56.6	1.3	
	c-axis projection: Ketcham et al. (2007), 5.5 M	Alpha calculation: redistribution	Present-day T range: 0-30^{o}C	Good: 2			
	kinetic parameters and initial length: from Dpar	Alpha age correction: Farley et al. (1996)	monotonic cooling				
JV1	Annealing model: Kectahm et al. (2007)	same as above	same as above	Acceptable: 45	45.1	1	
	c-axis projection: Ketcham et al. (2007), 5.5 M	Alpha calculation: redistribution	same as above	Good: 2			
	kinetic parameters and initial length: from Dpar	same as above	same as above				
PU1	Annealing model: Kectahm et al. (2007)	AHe calibration: Schuster et al. (2006) Do/a2	maximum T: 120^{o}C	Acceptable: 28	43.8	0.9	T of crystalization:
	c-axis projection: Ketcham et al. (2007), 5.5 M	Alpha calculation: static ejection	Present-day T range: 0-30^{o}C	Good: 6	41.6	0.7	69 Ma from U-Pb
	kinetic parameters and initial length: from Dpar	Alpha age correction: Farley et al. (1996)	monotonic cooling				
PK1 B	Annealing model: Kectahm et al. (2007)	NA	maximum T: 150^{o}C	Acceptable: 51	NA		
	c-axis projection: Ketcham et al. (2007), 5.5 M	NA	Present-day T range: 0-30^{o}C	Good: 7	NA		
	kinetic parameters and initial length: from Dpar	NA	monotonic cooling		NA		
AR5	NA	AHe calibration: Flowers et al. (in press)	maximum T: 140^{o}C	Acceptable: 756	49.96	2.85	
	NA	Alpha calculation: ejection	Present-day T range: 0-30^{o}C	Good: 49	53.24	2.81	
	NA	Alpha age correction: Farley et al. (1996)	monotonic cooling				
AR6	NA	AHe calibration: Schuster et al. (2006) Do/a2	maximum T: 140^{o}C	Acceptable: 972	55.69	1.63	
	NA	Alpha calculation: static ejection	Present-day T range: 0-30^{o}C	Good: 523			
	NA	Alpha age correction: Farley et al. (1996)	monotonic cooling				
AR3	NA	Flowers et al. (in press)	maximum T: 140^{o}C	Acceptable: 894	44.62	3.6	
	NA	Alpha calculation: redistribution	Present-day T range: 0-30^{o}C	Good: 579	44.5	2.83	
	NA	Alpha age correction: Farley et al. (1996)	monotonic cooling				
JV3	NA	Flowers et al. (in press)	maximum T: 140^{o}C	Acceptable: 831	42.54	1.7	
	NA	Alpha calculation: ejection	Present-day T range: 0-30^{o}C	Good: 446			
	NA	Alpha age correction: Farley et al. (1996)	monotonic cooling				
GT1	NA	Flowers et al. (in press)	maximum T: 140^{o}C	Acceptable: 370	45.2	1.05	
	NA	Alpha calculation: redistribution	Present-day T range: 0-30^{o}C	Good: 206			
	NA	Alpha age correction: Farley et al. (1996)	monotonic cooling				
PK5	NA	AHe calibration: Schuster et al. (2006) Do/a2			50.3	0.94	
	NA	Alpha calculation: static ejection			49.17	1.16	
	NA	Alpha age correction: Farley et al. (1996)					

For AFT ages refer to Table DR5

** not enough L for modeling

Italic indicates samples for which AFT and Ahe data are available and provided acceptable/good results

Sample id	Sample name	Latitude (°)	Longitude (°)	Elevation (m)	Mass (ug)	half-width (um)	U ppm	Th ppm	Sm ppm	4He (nmol/g)	HAC	Raw age (Ma)	Corrected age (Ma)	Estimated 1 sigma error (Ma)	eU ppm
6-4-06-1-1	AR1	33.25	85.19	5506	5.063	52.00	14.120	49.818	136.628	2.046	0.751	14.537	19.37	0.40	25.827
6-4-06-1-2	AR1	33.25	85.19	5506	1.100	31.75	9.902	23.949	102.148	0.888	0.583	10.481	17.97	0.78	15.530
6-12-06-6PK-1	PK6	33.30	85.17	5601	2.207	46.00	37.913	10.026	327.689	4.221	0.711	19.233	27.06	0.62	40.269
6-12-06-6PK-2	PK6	33.30	85.17	5601	8.511	78.50	31.796	9.350	223.197	4.299	0.825	23.237	28.16	0.63	33.994
6-20-06-2PK-1	PK5	31.50	89.08	4563	4.262	60.00	9.741	28.938	379.106	3.561	0.768	38.639	50.30	0.94	16.541
6-20-06-2PK-2	PK5	31.50	89.08	4563	1.337	34.50	9.774	30.852	398.059	2.922	0.626	30.795	49.17	1.16	17.024
6-20-06-3PK-1	PK3	31.41	89.02	4608	0.627	31.00	38.921	36.182	406.302	8.188	0.578	31.596	54.64	1.33	47.424
06GT64-1	GT1	33.25	85.19	5308	4.815	68.75	22.018	6.551	218.731	4.561	0.784	35.426	45.20	1.05	23.558
5-21-02-4b-2	AR2	33.20	86.74	5163	1.157	35.50	2.520	0.000	22.248	0.138	0.621	10.041	16.18	4.13	2.520
PK97-6-4-1A-1	PK1A	31.88	91.70	4706	0.742	30.75	28.376	6.588	38.818	10.259	0.567	63.181	111.50	3.03	29.924
PK97-6-4-1A-2	PK1A	31.88	91.70	4706	2.471	47.50	38.782	1.824	36.390	19.334	0.700	90.699	129.51	2.68	39.210
JV61204-3-1	JV3	31.50	84.50	4783	0.715	26.75	11.737	41.522	286.006	2.718	0.540	22.963	42.54	1.70	21.494
JV61204-3-4	JV3	31.50	84.50	4783	0.967	32.25	12.066	33.556	421.807	3.077	0.600	27.761	46.31	1.47	19.952
6-27-98-2b-1	AR3	33.76	84.56	4923	0.589	29.00	4.507	4.585	344.489	0.811	0.562	24.998	44.50	2.83	5.584
6-27-98-2b-2	AR3	33.76	84.56	4923	0.776	38.50	3.941	2.671	90.576	0.702	0.623	27.784	44.62	3.60	4.568
JV61504-4-1	JV4	31.36	89.89	5230	1.806	35.25	21.793	18.593	396.715	5.405	0.653	37.495	57.42	1.16	26.162
JV61504-4-2	JV4	31.36	89.89	5230	1.343	36.75	44.683	23.975	488.124	8.293	0.630	30.142	47.86	1.03	50.317
Sh7-12-03-02-3	SH2	30.07	91.14	4533	1.818	42.00	21.602	44.290	95.488	1.632	0.679	9.395	13.84	0.33	32.010
Sh7-12-03-02-2	SH2	30.07	91.14	4533	1.432	36.25	23.320	61.719	185.283	1.755	0.641	8.525	13.31	0.38	37.824
Sh7-12-03-02-4	SH2	30.07	91.14	4533	3.480	51.25	21.021	41.951	117.074	1.978	0.734	11.794	16.06	0.36	30.879
Sh7-12-03-02-5	SH2	30.07	91.14	4533	3.433	50.75	18.953	37.689	75.934	1.720	0.732	11.402	15.57	0.38	27.810
6-29-98-14b-1	AR4	33.87	84.12	4870	1.560	41.50	10.554	18.891	25.479	1.983	0.645	24.390	37.81	1.14	14.994
6-29-98-14b-2	AR4	33.87	84.12	4870	0.901	31.75	9.201	25.193	36.696	1.837	0.568	22.361	39.34	1.66	15.122
6-29-98-14b-4	AR4	33.87	84.12	4870	0.979	30.75	9.011	19.547	26.318	1.527	0.593	20.693	34.92	1.17	13.605
PK-97-6-4-3A-1	PK3A	32.12	91.71	4762	2.115	48.00	27.987	18.940	143.043	7.877	0.685	44.627	65.13	1.35	32.438
PK-97-6-4-3A-2	PK3A	32.12	91.71	4762	1.880	39.25	37.202	27.253	221.089	8.727	0.676	36.773	54.38	1.19	43.606
PK97-6-4-3A-3	PK3A	32.12	91.71	4762	3.342	54.25	35.581	28.415	154.817	9.522	0.745	41.452	55.66	1.14	42.259
PK97-6-4-3A-4	PK3A	32.12	91.71	4762	2.684	46.75	33.083	25.315	245.977	7.090	0.698	33.335	47.74	0.99	39.032
JV61504-1-1	JV1	31.34	89.88	5110	2.267	42.75	61.280	14.692	426.344	10.859	0.683	30.807	45.12	1.03	64.732
JV61504-1-2	JV1	31.34	89.88	5110	1.332	34.25	65.141	21.957	487.814	10.565	0.640	27.590	43.08	0.95	70.300
JV61504-1-3	JV1	31.34	89.88	5110	1.291	35.25	82.007	25.487	544.731	13.844	0.624	28.907	46.34	0.98	87.996
5July104-1	PU1	33.25	92.01	5591	3.588	49.75	43.497	106.407	497.987	12.145	0.738	32.439	43.95	0.73	68.503
5July104-2	PU1	33.25	92.01	5591	0.692	31.25	60.517	99.110	604.044	11.651	0.581	25.471	43.84	0.91	83.808
5July104-3	PU1	33.25	92.01	5591	2.567	43.75	44.654	105.516	482.480	11.018	0.698	29.048	41.61	0.72	69.450
6-15-98-PK6-1	AR5	32.78	84.02		0.622	28.75	9.609	12.993	114.867	1.940	0.561	28.016	49.96	2.85	12.663
6-15-98-PK6-2	AR5	32.78	84.02		1.116	37.50	6.024	7.719	96.983	1.469	0.641	34.117	53.24	2.81	7.838
6-23-98-PK1A-1	AR6	32.71	84.24		0.871	32.25	15.564	27.957	209.417	4.043	0.599	33.356	55.69	1.63	22.134
6-23-98-PK1A-2	AR6	32.71	84.24		1.462	38.50	28.925	36.887	251.124	6.217	0.659	30.322	46.02	1.05	37.594
6-23-98-PK1A-3	AR6	32.71	84.24		1.215	33.25	23.527	37.851	258.168	5.345	0.622	30.167	48.53	1.13	32.422

footnote: half-width is c-ax is perpendicular half-width

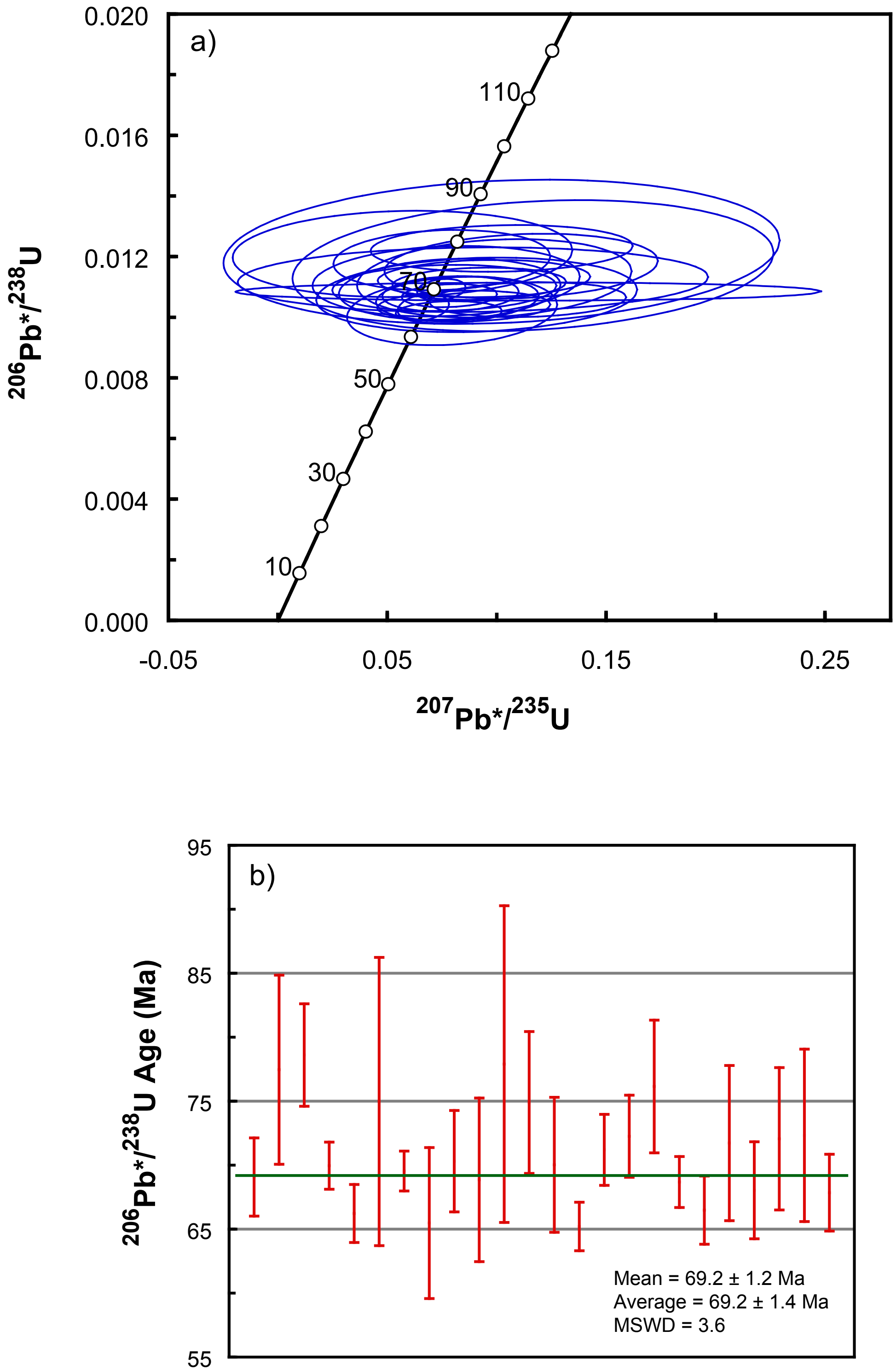

Figure DR1. U-Pb plots for sample PU1. All uncertainties are at the 2-σ level. a) Condordia plot of all analyzed zircons. b) Weighted average of $^{206}Pb/^{238}U$ ages. Green bar represents the mean. The "Mean" age only includes random uncertainties; the "Average" age includes random and systematic uncertainties and is the reported age for this sample.

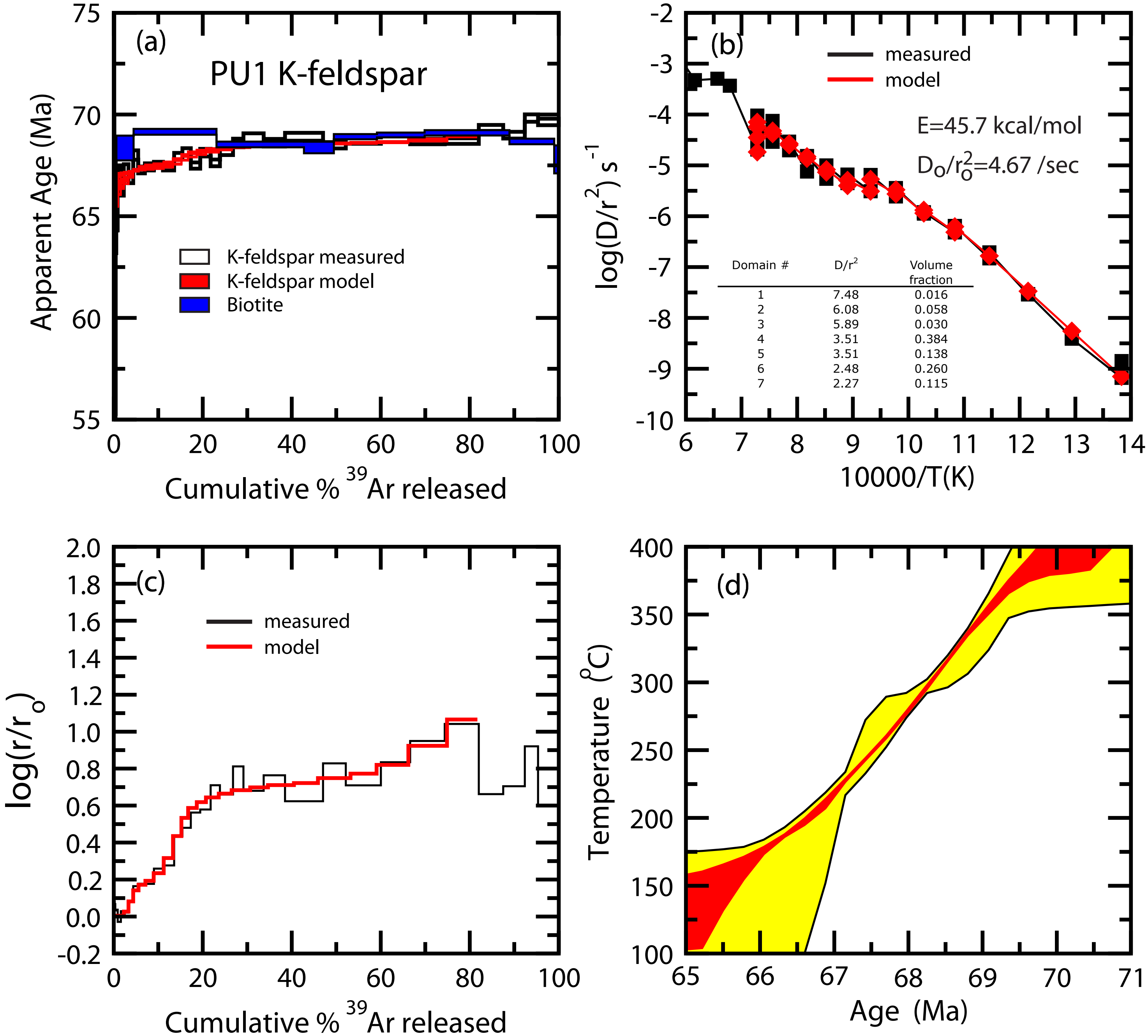

Figure DR2. K-feldspar MDD and biotite results. a) age spectra for biotite and K-feldsar. b) Arrhenius plot, c) Log (r/r_o) plot, and d) calculated thermal history assuming only cooling from an initially high temperature.

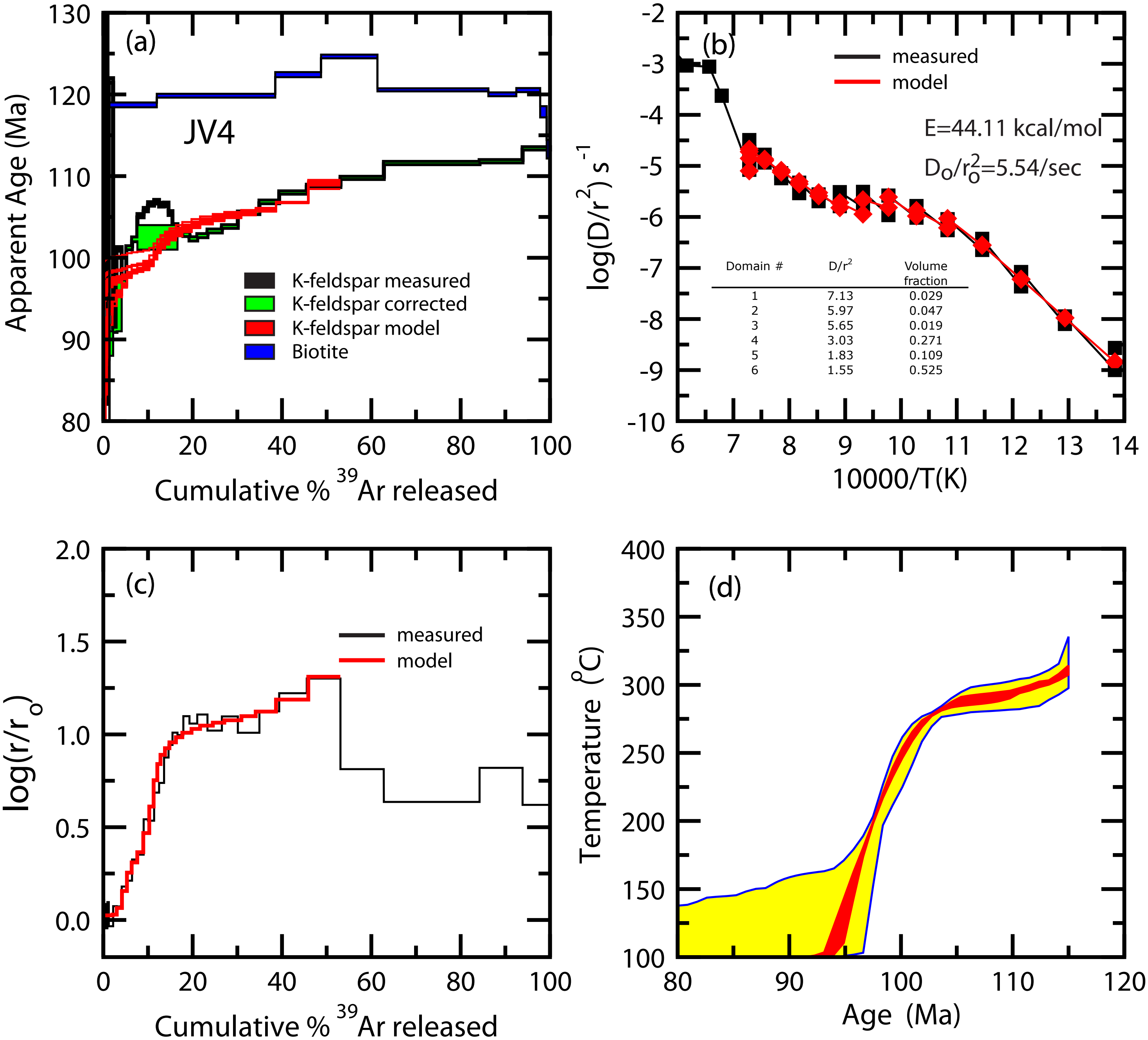

Figure DR3. K-feldspar MDD and biotite results. a) age spectra; green boxes represent a spectrum that removes the intermediate age hump from the measured spectrum. b) Arrhenius plot, c) Log (r/r_o) plot, and d) calculated thermal history assuming only cooling from an initially high temperature.

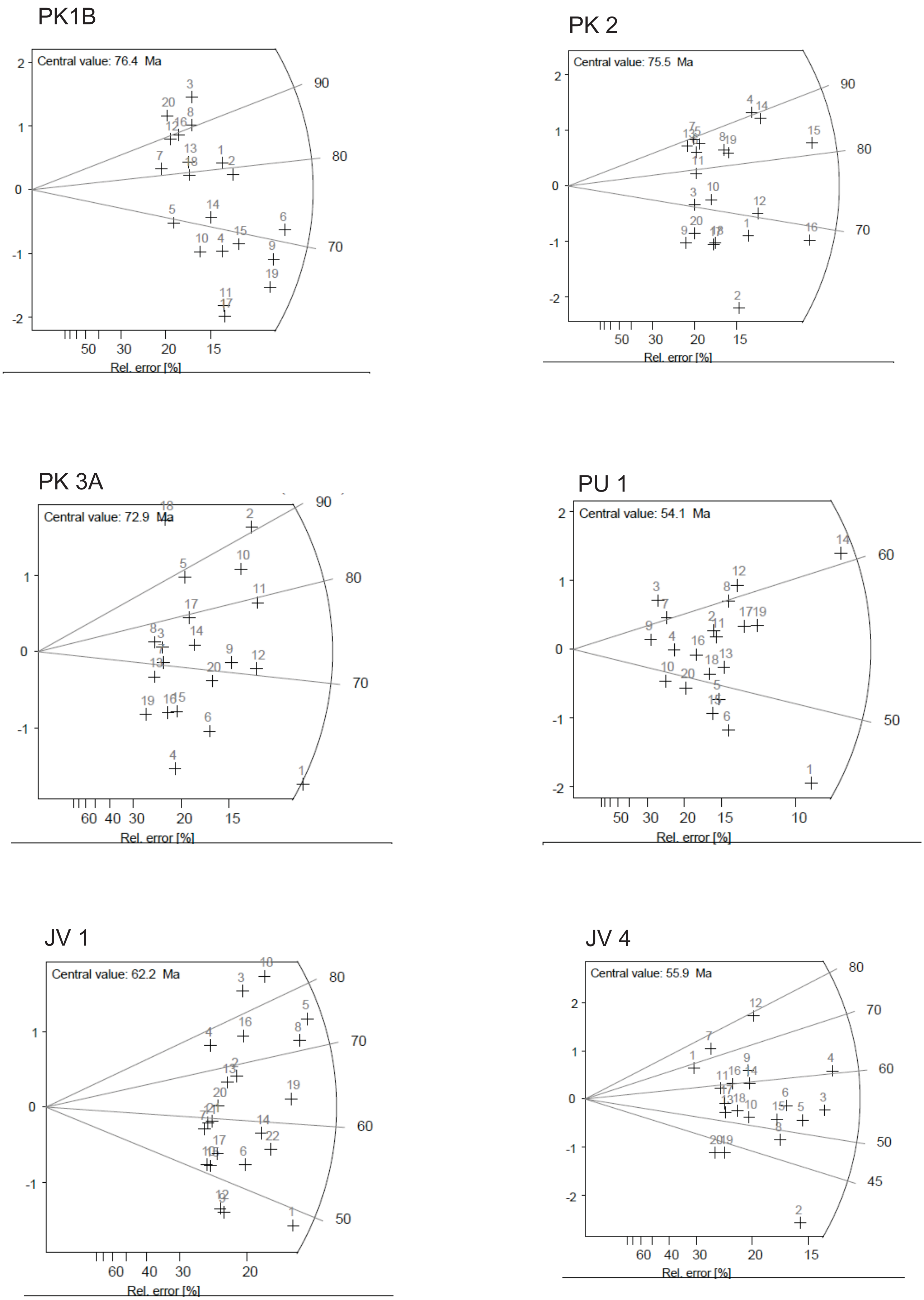

Figure DR4 AFT radio-plots for samples listed in Table DR5

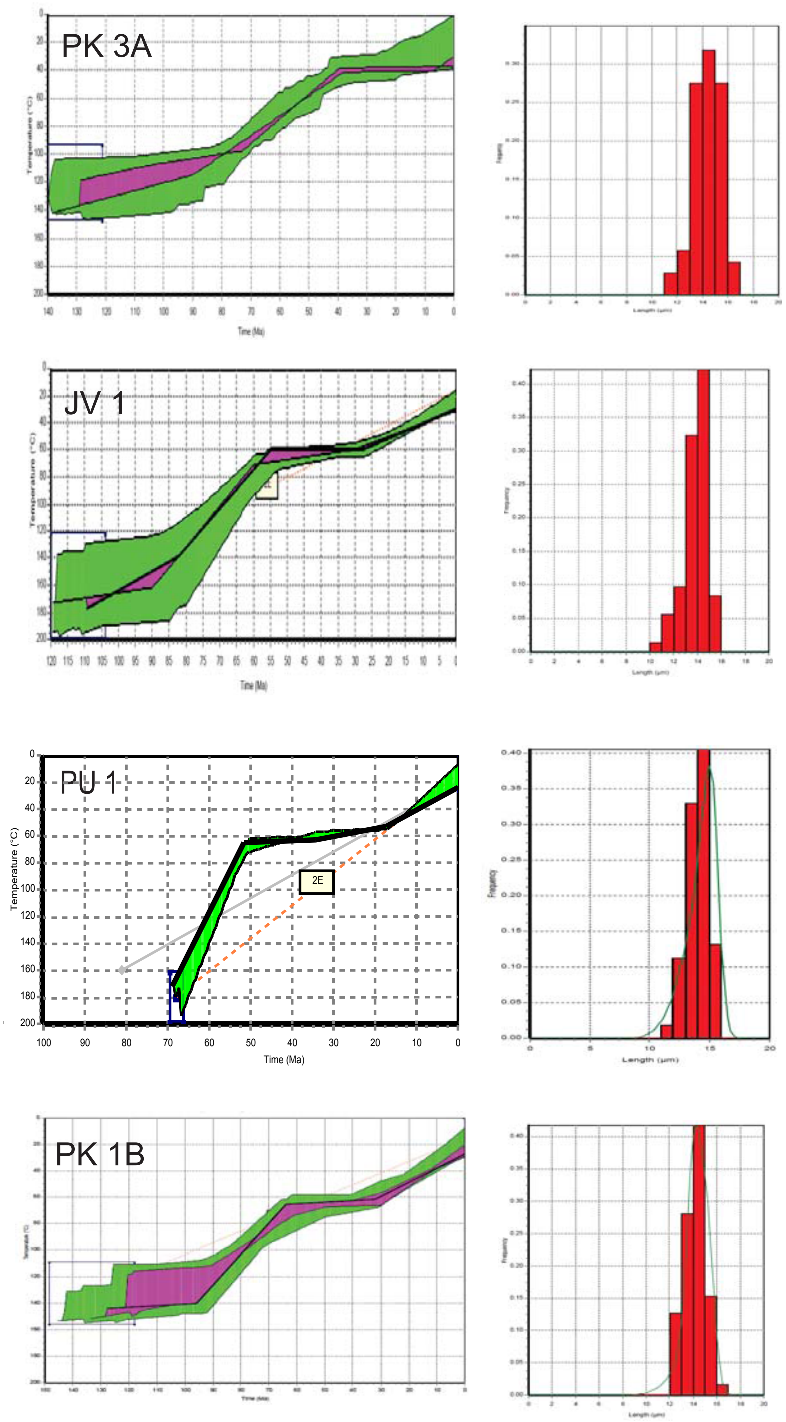

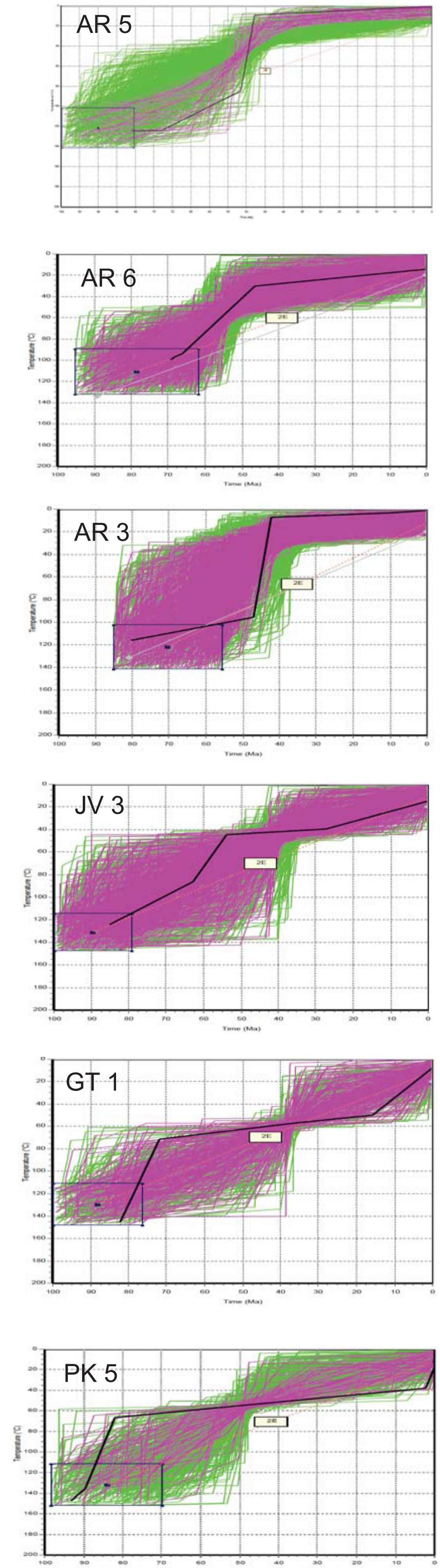

Figure DR5. HeFTy thermal modeling results